Classification of brain states across the awake-sleep transition in the cortex of rats

Sancristóbal, B.[1],Torao-Angosto, M.[2], Sanchez-Vives, M. V.[2,3], Moreno-Bote, R.[1]

[1]*Center for Brain and Cognition & Department of Information and Communication Technologies (UPF), Barcelona, Spain;*
[2]*Systems Neuroscience, Institut d'Investigacions Biomèdiques August Pi i Sunyer (IDIBAPS), Barcelona, Spain;*
[3]*ICREA (Institució Catalana de Recerca i Estudis Avançats), Barcelona, Spain.*

Recent findings have revealed that changes in consciousness levels correspond to changes in the interactions between functionally specialized brain regions [1]. Therefore, differences across brain states not only arise locally, but are also manifested in the effective connectivity among widespread cortical areas. Indeed, local dynamics fail to explain differences between wakefulness and rapid eye movement (REM) sleep, since, at this stage, cortical activity exhibits awake-like dynamics but the sensory threshold is raised above waking levels similar to NREM sleep. In this study we focused on **natural sleep**, and we have recorded cortical local field potentials (LFP) of rats while they naturally transitioned from wakefulness to sleep and vice-versa.

Scoring arousal levels is a time-consuming task. Besides, the wake-sleep cycle of rodents is more fragmented than in humans and the presence of REM epochs is lower [2]. Automatic scoring programs that have been published to date are mainly based on decision trees that require threshold criteria for the choice of sleep-wake states [3,4] or on naive Bayes classifiers [5]. **Here we present a classification algorithm that can facilitate state detection in chronic animal experiments that last several days. Moreover, reliable online identification of brain states allows simultaneous computations of effective connectivity estimates across recording sites, which provide an online large-scale description of those states.**

1 Experimental data

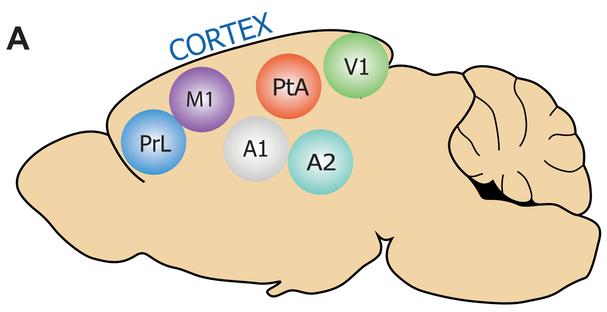

Extracellular local field potential (LFP) recordings from PrL, M1, PtA, A1, A2 and V1, were obtained in awake freely-moving (N=2) Lister-Hooded rats (Fig.1).

- PrL - Prelimbic cortex
- M1 - Primary motor cortex
- V1 - Primary visual cortex
- A1 - Primary auditory cortex
- A2 - Secondary auditory cortex
- PtA - Parietal association area

The electromyogram (EMG) and the position of the rat were also monitored.

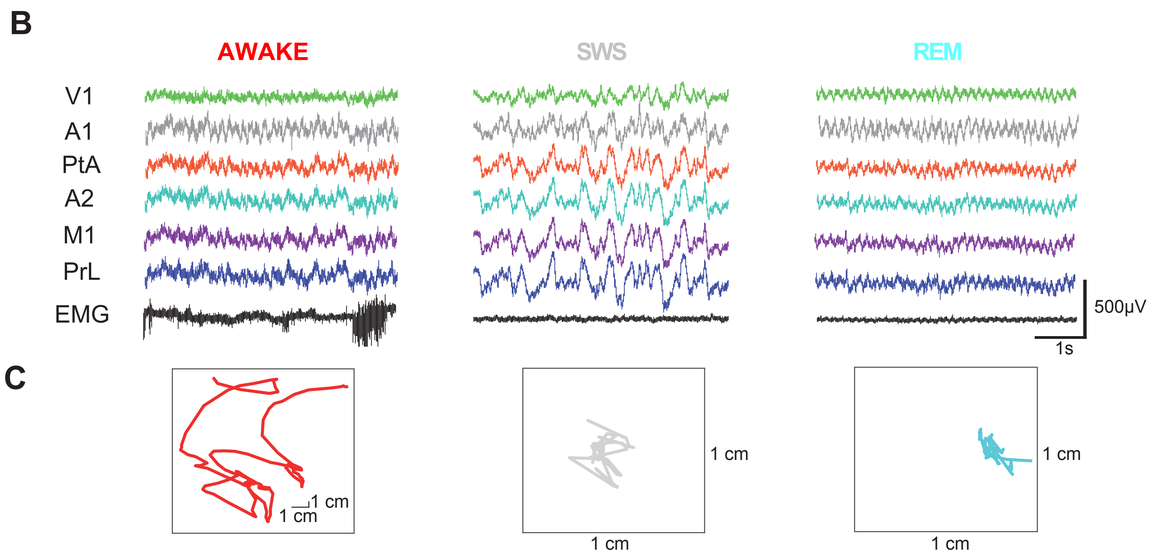

Figure 1 (A) Scheme of recorded cortical areas. **(B)** Raw LFP signal (color) in PrL, M1, PtA, A1, A2 and V1 and EMG (black) for a baseline recording of (left) an awake and freely moving rat, (middle) during slow wave sleep (SWS) and (right) during rapid-eye-movement (REM). The bottom panels show the trajectory of the rat during the same interval. **(C)** Trajectory of the rat.

2 Power spectral density, EMG fluctuations and mean displacement during different brain states

We found that power spectral density ratios of beta – gamma (β, 20-30Hz – γ, 30-80Hz) and theta – delta (θ, 5-10Hz – δ, 1-5Hz) in 5 s epochs can be successfully used as predictors to classify the three states. Training of the classifier is performed offline in order to reduce the distance between the predictions and the manual classification (ground truth). The parameters that minimize such cost function define the boundaries that separate the states in the feature space.

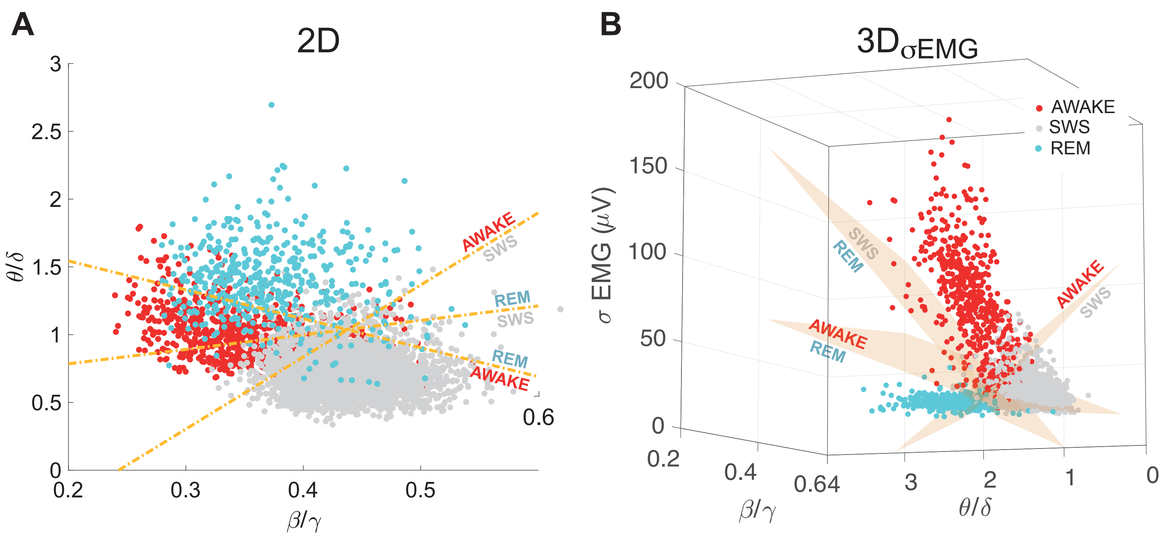

Figure 2 (A) Power spectral ratios during different brain states. **(B)** Power spectral rations against the standard deviation of the EMG. Each dot represents a 5 s window of recordings. Orange boundaries are computed after training a multinomial logistic regression (see section 3) on the manually classified segments.

3 Multinomial logistic regression classifier

We tested the performance of the classifier with different choices of features. EMG fluctuations, σEMG, increase the accuracy of the predictions of the 2D model. However, average displacement, <R>, does not unequivocally define brain states, but rather movement and stillness.

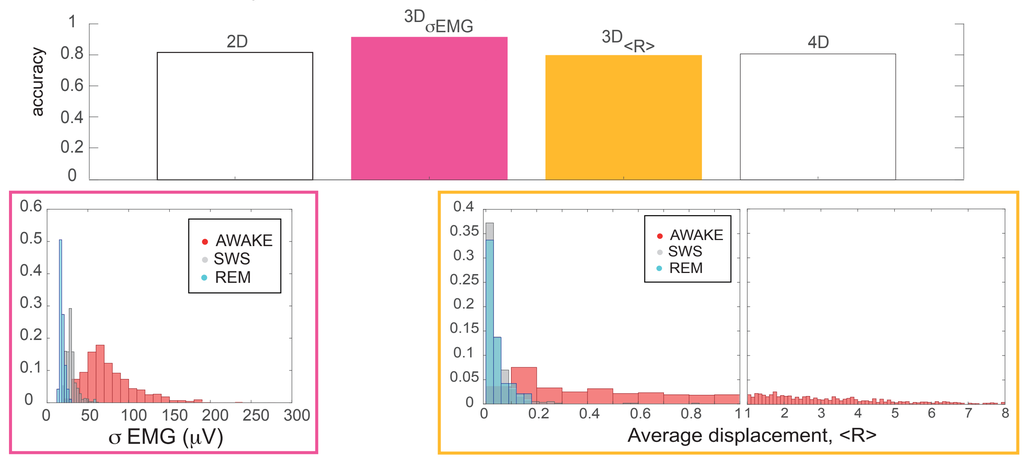

Figure 3 Accuracy of the predictions. The accuracy of the classifier was computed over a new data set of the freely moving rat. The highest performance is obtained for a 3D model that combines the spectral content of the LFP and the fluctuations of the EMG.

4 Functional connectivity: Phase coherence in gamma between different cortical sites, brain states and frequencies

We investigated whether the functional connectivity between the recorded cortical areas depended on the brain state. Phase coherence, $C_{xy}(f)$, estimates phase synchronization from Fourier's phase (computed every 250 ms) independently for each frequency [6].

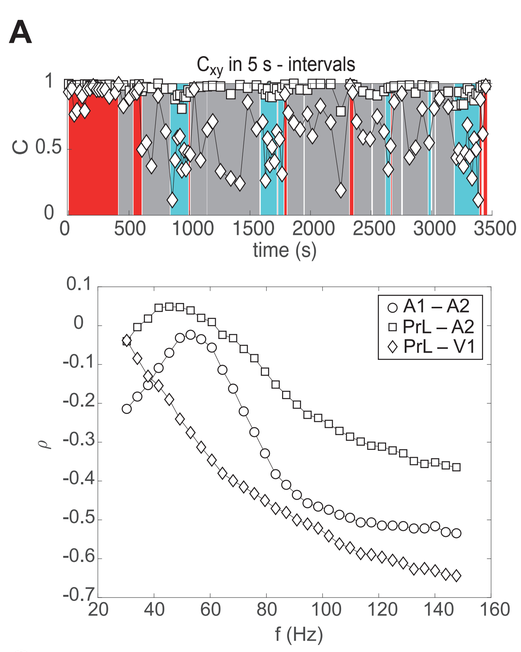

$$C_{xy}(f) = \frac{1}{N}\sum_{n}^{N}\frac{S_{xy}(f,n)}{|S_{xy}(f,n)|}$$

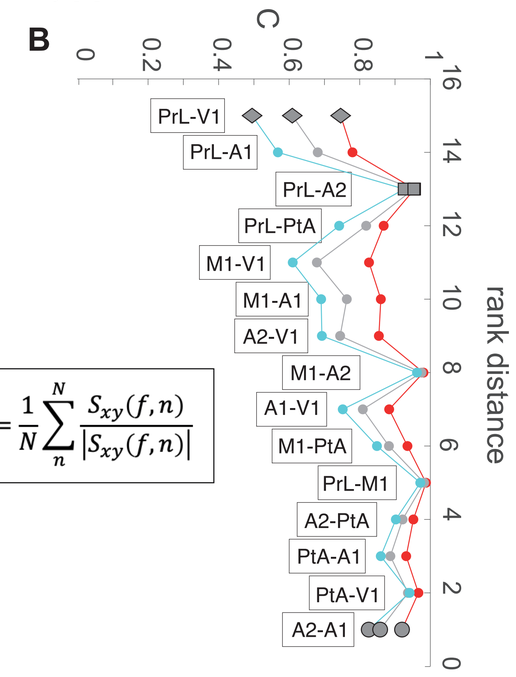

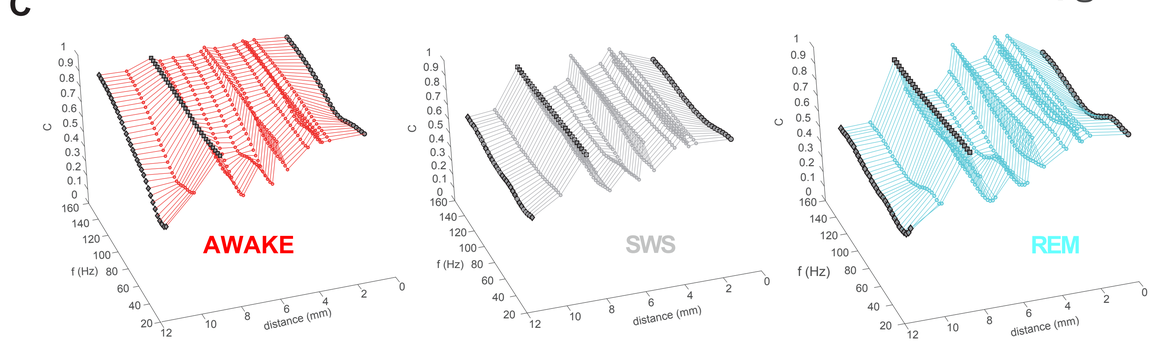

Figure 4 Phase coherence in the gamma band. (A) *Top*. Phase coherence at 150 Hz across time between two pairs of electrodes and the brain states detected beneath. *Bottom*. Cross-correlation, ρ, between phase coherence and the time course of brain states within the gamma band between pairs of electrodes. **(B)** Average phase coherence within 30 - 150 Hz for all 3 states. **(C)** Mean phase coherence during (left) awake, (middle) SWS and (right) REM for all pairs of electrodes.

5 Conclusions

We used a classification algorithm to perform an automatic online detection of brain states, namely awake, slow wave sleep (SWS) and REM. The highest accuracy is obtained using three features to characterise these states: the beta-gamma and theta-delta power spectral density ratios of the LFP and the standard deviation of the EMG.
We used a measure of temporal phase coherence, C, in the gamma band to quantify changes in functional connectivity across brain states. We found that, on average, C decreases from awake to SWS and is lowest in REM. Although there is a general decrease in C as the distance between pairs of electrodes increases, certain pairs are insensitive to brain states (i.e. PrL-A2), while others modulate C accordingly (i.e. PrL-V1).

References: **[1]** Stitt I, Hollensteiner K J, Galindo-Leon E, Pieper F, Fiedler E, Stieglitz T, Engler G, Nolte G, Engel A K (2017) Sci Rep. 7:8797. **[2]** Bastianini S, Berteotti C, Gabrielli A, Lo Martire V, Silvani A, Zoccoli, G. (2015) Arch Ital Biol. June-Sep; 153(2-3):58-66. **[3]** Hamrahi H, Chan B, Horner R L (2001) J Appl Physiol. 90:2130-2140. **[4]** Louis RP, Lee J, Stephenson R (2004) J Neurosci Methods. Feb 15; 133(1-2): 71-80. **[5]** Rytkönen KM, Zitting J, Porkka-Heiskanen T. (2011) J Neurosci Methods. Oct 30; 202(1):60-4. **[6]** Womelsdorf T, Schoffelen, JM, Oostenveld R, Singer W, Desimone R, Engel A K, Fries P (2007) *Science* 316, 1609.

B. Sancristóbal has received financial support through the Postdoctoral Junior Leader Fellowship Programme from "la Caixa" Banking Foundation. This work was funded by the Spanish Ministry of Science (BFU2017-85048-R) and by EU H2020 Research and Innovation Programme, Grant 720270 (HBP SGA2).